

A Wiener process perspective on local intrinsic dimension estimation methods

Piotr Tempczyk^{1,2,3}, Łukasz Garncarek^{3,4}, Dominik Filipiak^{5,6,7}, and Adam Kurpisz^{3,8,9}

¹Institute of Informatics, UW

²NASK

³PL4AI

⁴Snowflake

⁵Adam Mickiewicz University, Poznań

⁶Perelyn

⁷University of Innsbruck

⁸BFH Bern Business School

⁹ETH Zurich

Abstract

Local intrinsic dimension (LID) estimation methods have received a lot of attention in recent years thanks to the progress in deep neural networks and generative modeling. In opposition to old non-parametric methods, new methods use generative models to approximate diffused dataset density and scale the methods to high-dimensional datasets like images. In this paper, we investigate the recent state-of-the-art parametric LID estimation methods from the perspective of the Wiener process. We explore how these methods behave when their assumptions are not met. We give an extended mathematical description of those methods and their error as a function of the probability density of the data.

1 Introduction

LID estimation has gained increasing attention in recent years as part of the fast-growing field of topological data analysis. It was able to progress from non-parametric methods to parametric ones thanks to the latest progress in the field of generative modeling. LID estimation methods are algorithms for estimating the manifold's dimension from which the data point x was sampled. In those methods, we assume that the data lie on the union of one or more manifolds that may be of different dimensions.

The estimation of intrinsic dimension is a critical issue in data analysis and machine learning (Ansuini et al., 2019; Li et al., 2018; Rubenstein et al., 2018) and was investigated in relation to dimensionality reduction and clustering (Vapnik, 2013; Kleindessner and Luxburg, 2015; Camastra and Staiano, 2016), analyzing the training and representation learning processes within deep neural networks (Li et al., 2018; Ansuini et al., 2019; Pope et al., 2020; Loaiza-Ganem et al., 2024), verifying the union of manifolds hypothesis for images Brown et al. (2022), and used to improve out-of-distribution detection algorithm Kamkari et al. (2024a).

Before Tempczyk et al. (2022), two approaches were presented to solve the intrinsic dimension estimation problem, both based on non-parametric methods. The first approach employs global methods such as PCA and its variants; see, e.g., Fukunaga and Olsen (1971); Minka (2000); Fan et al. (2010). These methods are known to suffer from issues related to a manifold curvature and non-uniformity of the data distribution. They also assumed that data lies on a single manifold of constant dimension, so dimensionality is the same for all x . The second approach is based on local methods that explore the geometric properties of neighborhoods Johnsson et al. (2014); Levina and Bickel (2004) calculating some statistics using points from the neighborhood of x . Although all aforementioned methods perform reasonably well for a small number of dimensions, the higher dimensionality affects their performance Tempczyk et al. (2022); Campadelli et al. (2015); Camastra and Staiano (2016).

Very recently, a new approach emerged for the local methods, which is based on a two-step procedure. In the first step, the dataset is perturbed with some noise, and in the second step, its dimensionality is estimated using various techniques. These include generative models to analyze changes in density Tempczyk et al. (2022); Kamkari et al. (2024a) or in singular values of the Jacobian Horvat and Pfister (2022, 2024) for different noise magnitudes, and analyzing rank of scores from diffusion model as mentioned in Stanczuk et al. (2024).

Although the new algorithms provide state-of-the-art performance for large and real-life data sets, it is crucial for their performance that adding noise to the data set is an injective process, which means that the resulting densities after adding noise uniquely identify the original distribution of the data set. Otherwise, it is impossible to neither uniquely reverse the process nor analyze the original structure of the data set. One example in the theoretical model that does not admit such a problem is a flat manifold with a uniform distribution of data points. In such a case those algorithms perform best, as showed in experimental results. In other cases, a hypothetical line of attack would be to decrease the magnitude of noise added to the data set so that the manifold is approximately flat and uniform in the scale of the noise magnitude. This, however, is not possible in practice for several reasons. One is that data is often a set of discrete points (especially in the case of audio and visual data), and considering the noise of much smaller magnitude than the minimum distance between points does not lead to any meaningful process. Moreover, neural net training is done with finite precision and the stochastic gradient descent procedure introduces noise

to the density estimates, so very small changes in density cannot be observed in practice, which may lead to poor quality estimates of LID.

In this paper, we point out and exploit the fact that adding Gaussian noise of varying magnitudes can be seen as studying the evolution of the Wiener process describing the diffusion of particles (points of the dataset) in space. This point of view enables us to employ Fick’s Second Law of Diffusion to eliminate time derivatives from mathematical descriptions of state-of-the-art LID algorithms Tempczyk et al. (2022); Kamkari et al. (2024a), and replace them with spatial derivatives. Such considerations can be taken into account in the second step of the considered algorithms, leading to more accurate results.

Contribution

1. We explore the first step of existing algorithms in the language of Wiener process and calculate important cases of diffusion from lower-dimensional manifolds with non-uniform probability density into higher dimensional ambient space.
2. We recognize and define new categories (isolated and holistic algorithms) for the Wiener process based parametric LID estimation algorithm family and categorize existing algorithms accordingly.
3. We derive closed-form expressions for crucial parameters used in two state-of-the-art isolated LID estimation algorithms as a function of on-manifold density and manifold dimensionality, which can be viewed as closed-form expression for deviation from flat manifold with uniform distribution case for them.

2 Related work

The review of non-parametric methods for local and global intrinsic dimension estimation can be found in Campadelli et al. (2015); Camastra and Staiano (2016), and a broad comparison of those methods on bigger datasets (in terms of dimensionality) can be found in Tempczyk et al. (2022).

Although we do not analyze non-parametric methods in this paper, the interesting and worth mentioning recent work on non-parametric LID estimation is Bailey et al. (2022). Authors explore the connection of LID to other well-known measures for complexity: entropy and statistical divergences and develop new analytical expressions for these quantities in terms of LID. The same authors in their follow-up paper Bailey et al. (2023) establish the relationships for cumulative Shannon entropy, entropy power, Bregman formulation of cumulative Kullback–Leibler divergence, and generalized Tsallis entropy variants, and propose four new estimators of LID, based on nearest neighbor distances.

2.1 Parametric methods for LID estimation

During the last few years many parametric methods for estimating LID emerged. In Zheng et al. (2022) the authors prove that VAE are capable of recovering the correct manifold dimension and demonstrate methods to learn manifolds of varying dimension across the data sample. Authors of Yeats et al. (2023) connects the adversarial vulnerability of score models with the geometry of the underlying manifold they capture. They show that minimizing the Dirichlet energy of learned score maps boosts their robustness while revealing LID of the underlying data manifold.

Wiener process based algorithms Among parametric methods, there is a group of algorithms, that have one thing in common: they simulate a Wiener process on a dataset and directly use some properties of time evolving density to estimate LID. We can divide those algorithms into three groups:

1. **LIDL** Tempczyk et al. (2022) and its efficient and most accurate implementation using diffusion models called **FLIPD** Kamkari et al. (2024b). These algorithms use the rate of change of the probability density at point x during the Wiener process to estimate LID at x . For small diffusion times t the logarithm of a density is a linear function of a logarithm of t , and the proportionality coefficient is equal $d - D$ for small t , where d is manifold density and D is ambient space dimensionality. Authors of FLIPD show, that their algorithm is efficient and our experiments show, that is more scalable than algorithms from the second group (and with high probability more accurate, but there is a lack of comparison between FLIPD and methods from second group) and more accurate than algorithms from the third group, which led us to the conclusion that at this moment this family of algorithms is state-of-the-art in LID estimation.
2. **ID-NF** Horvat and Pfister (2022) (using normalizing flows), and the follow-up paper Horvat and Pfister (2024) **ID-DM** (using diffusion models) algorithms analyze how a singular values of a Jacobian of a function transforming a standard normal distribution into a diffused dataset at x evolves during the Wiener process. Authors use an observation, that when transforming a d -dimensional manifold into a D -dimensional Gaussian we have to expand space more in the off-manifold directions, especially for small diffusion times t .
3. The third group, for now, is composed of one algorithm: Stanczuk et al. (2024). We will call this algorithm **NB** – Normal Bundle – following the convention from Kamkari et al. (2024b). Authors of NB make an observation, that for small diffusion times t the score function from the Score-based diffusion model Song et al. (2020) lies in the normal space to the manifold at x . The procedure is the following: calculate the score function for a bunch of diffused versions of x for a fixed diffusion time t , stack them as column vectors into a matrix S , and estimate the rank of S , which is then used as an estimate of $D - d$.

3 Isolated and holistic algorithms

In this work we are going to take a closer look at the Wiener process based algorithms described in the last paragraph of Section 2. Although all of those algorithms apply a Wiener process to the dataset during their first phase, when looking at their second phase, we can divide them into two groups: isolated (LIDL, FLIPD, NB) and holistic (ID-NF, ID-DM). The intermediate results of the first group used to calculate LID use only (assuming that a generative model approximates diffused data distribution ρ_t perfectly) information about the shape of the data probability density function (without normalization constant). Their estimate depends on the gradient of the logarithm of ρ_t around x (NB) or $d \log \rho_t / d \log t$ at x (LIDL, FLIPD). Because in practice ρ_t is a function of the values of original data distribution p_S in a ball of radius $r \approx 4\sqrt{t}$ around x in the data space. What the values of p_S outside this ball are do not matter in practice for isolated algorithms because the diffused particles in the Wiener process can travel longer distances than r with very low probability (less than $3.7 \cdot 10^{-5}$). When we add some new data points to the dataset far away from x , it doesn't change the shape of ψ close to x (this operation only changes a normalization constant, which becomes 0 after taking a logarithm of ψ and taking a derivative).

The holistic algorithms work quite differently. In the case of ID-NF and ID-DM, they calculate singular values of the Jacobian of the function $\zeta : \mathbb{R}^N \rightarrow \mathbb{R}^N$ transforming ρ_t into a standard normal distribution. This ζ function strongly depends on the entire shape of ρ_t . When we change ρ_t far away from x we don't change the shape of ρ_t close to x . The same is not true for $\zeta(x)$. When we add many data points to the dataset far away from x and we keep the latent distribution fixed we have to change the way we compress and stretch the space to match the new distribution. This property makes the analysis of the behavior of ID-NF and ID-DM much harder (maybe even impossible) as a function of density evolution around x .

To give an illustrative example of this behavior let's imagine that our dataset is one-dimensional and consists of 10K points sampled from $\mathcal{N}(0, 1)$. Because we are transforming it into $\mathcal{N}(0, 1)$, ζ is an identity function. Now let's add to the dataset another 10K points sampled from $\mathcal{N}(100, 1)$. Now we have to stretch our space in some areas to transform one density into another and our ζ function (and its Jacobian) is far from being an identity function.

This approach can be extended for new algorithms in the future, and similar analysis can be carried out for the new algorithms from isolated group if only some intermediate results used to calculate LID can be expressed in the analytical form.

4 Wiener process perspective on LID estimation

Wiener process is a stochastic process modeling particle diffusion. Its increments over disjoint time intervals are independent and normally distributed, with variance proportional to time increments. Since in the machine learning community

the term *diffusion* is already overloaded, we will stick to Wiener process when speaking of particle diffusion process.

In this section we present a new perspective on perturbing datasets, unifying the approaches seen in the algorithms presented in Tempczyk et al. (2022); Stanczuk et al. (2024); Horvat and Pfister (2022, 2024); Kamkari et al. (2024b). As already mentioned, all these algorithms consist of two stages, the first of which amounts to perturbing the dataset with normally distributed random noise of fixed variance t . In the second stage, each of the algorithms utilizes the behavior of the perturbed density in the neighborhood of a fixed point under changes of the noise variance.

The first phase of each algorithm can be interpreted as applying the Wiener process to the points in the dataset. Afterward, the resulting set of points is used to train a generative model (depending on the chosen algorithm) to estimate the distribution of the dataset undergoing the Wiener process at time t . From the point of view of differential equations, the distribution density function of the diffused dataset is described by Fick’s Second Law of Diffusion.

Fick’s Second Law of Diffusion. *Let $\rho_t : \mathbb{R}^D \mapsto \mathbb{R}$ denote the probability density function modeling particles undergoing diffusion at time t . Then ρ_t satisfies the differential equation*

$$\frac{d}{dt}\rho_t = C\Delta\rho_t, \tag{1}$$

where $C \in \mathbb{R}$, and Δ stands for the standard Laplacian in \mathbb{R}^D .

Now, let us get to the specifics. Given a dataset embedded in \mathbb{R}^D , we assume that it has been drawn from some latent union of submanifolds S endowed with a probability measure p_S (which can be naturally treated as probability measure on \mathbb{R}^D). The goal of Local Intrinsic Dimension estimation is to find out the dimension of S at any point of the dataset.

To model the Wiener process with initial distribution p_S (which is not a function on \mathbb{R}^D), let us first define

$$\phi_t^D(x) = (2\pi t)^{-D/2} e^{-\|x\|^2/2t}. \tag{2}$$

This is the density of normal distribution on \mathbb{R}^D with covariance matrix tI . It is the fundamental solution of the differential equation given by Fick’s second Law of Diffusion (1) with $C = 1/2$. In our context, this means that the convolution

$$\rho_t = p_S * \phi_t \tag{3}$$

is the solution of (1) for $t > 0$ and hence it describes the Wiener process starting from the initial probability distribution p_S .

To limit the complexity introduced by curvature, we will consider from now on only flat manifolds. This means that, without loss of generality, we may assume that S is the first factor in product decomposition $\mathbb{R}^D = \mathbb{R}^d \times \mathbb{R}^{D-d}$. We will denote the coordinates of \mathbb{R}^d and \mathbb{R}^{D-d} by x and y , respectively. If we

moreover assume that p_S , now a probability distribution on \mathbb{R}^d , has a density $\psi: \mathbb{R}^d \rightarrow \mathbb{R}$, we can separate variables in (3), obtaining

$$\rho_t(x, y) = (\psi * \phi_t^d)(x) \phi_t^{D-d}(y) \quad (4)$$

for $(x, y) \in \mathbb{R}^d \times \mathbb{R}^{D-d}$.

The decomposition $\mathbb{R}^D = \mathbb{R}^d \times \mathbb{R}^{D-d}$ gives rise to the decomposition of the Laplacian on \mathbb{R}^D into Laplacians on the factors, namely $\Delta = \Delta_x + \Delta_y$, by simply grouping the derivatives with respect to x_i and y_i coordinates.

Lemma 4.1. *For $t > 0$ and $x \in \mathbb{R}^d$ we have*

$$\Delta \rho_t(x, 0) = \frac{d-D}{t} \rho_t(x, 0) + (2\pi t)^{(d-D)/2} \Delta_x (\psi * \phi_t^d)(x). \quad (5)$$

Proof. By using the product decomposition (4), we get

$$\Delta \rho_t(x, y) = (\psi * \phi_t^d)(x) \Delta_y \phi_t^{D-d}(y) + \Delta_x (\psi * \phi_t^d)(x) \phi_t^{D-d}(y) \quad (6)$$

Since $\phi_t^{D-d}(0) = (2\pi t)^{(d-D)/2}$, we obtain

$$\Delta_x (\psi * \phi_t^d)(x) \phi_t^{D-d}(0) = (2\pi t)^{(d-D)/2} \Delta_x (\psi * \phi_t^d)(x), \quad (7)$$

which corresponds to the second term of (5).

To derive the first term, we note that a direct computation yields the following.

$$\Delta_y \phi_t^{D-d}(y) = \phi_t^{D-d}(y) \left(\frac{\|y\|^2}{t^2} + \frac{d-D}{t} \right). \quad (8)$$

Evaluating this at $y = 0$ provides the desired result. \square

Let us stop here for a moment to discuss the expression $\Delta_x (\psi * \phi_t^d)$. When applying a differential operator to a convolution, under certain regularity conditions we can move it to either of the factors, which can turn out to be quite helpful. As it will turn out in the examples, $\Delta_x \psi * \phi_t^d$ will be the most desired form of $\Delta_x (\psi * \phi_t^d)$.

More precisely, given a convolution $f * g$, and a k -th order differential operator L , the following conditions guarantee that $L(f * g) = Lf * g$ (conditions for the other equality follow from commutativity of convolution):

1. All partial derivatives of f up to order k (including 0-th order, i.e. f itself) exist and are bounded.
2. The function g is integrable, i.e. $\int |g| < \infty$.

The second condition is clearly satisfied by densities of probability distributions, and ϕ_t^d satisfies the first condition. Hence, for any ψ we can write

$$\Delta_x (\psi * \phi_t^d) = \psi * \Delta_x \phi_t^d. \quad (9)$$

The second equality however requires additional assumptions;

$$\Delta_x (\psi * \phi_t^d) = \Delta_x \psi * \phi_t^d, \quad (10)$$

holds if ψ is bounded and has bounded partial derivatives up to order 2.

5 From Wiener process to LID estimation in LIDL

We are going to use results from the last section to analyze how the first family of algorithms (Tempczyk et al., 2022; Kamkari et al., 2024b) behaves for some particular cases. Because the main contribution from authors of Kamkari et al. (2024b) is a substantial improvement on the side of density estimation, from the theoretical perspective when dealing with perfect density estimators, both algorithms estimate the same quantity and give the same results. This is the reason from now on we will be analyzing LIDL because we want to analyze the aspects of those implementations that do not depend on the problems with density estimation itself.

Given a point $x \in S$ and a set of times t_1, \dots, t_n , LIDL estimates the linear regression coefficient α of the set of points $(\log \delta_i, \log \rho_{t_i}(x))$, where $\delta_i = \sqrt{t_i}$. It is proved in Tempczyk et al. (2022) that

$$\log \rho_t(x) = (d - D) \log \sqrt{t} + O(1), \quad (11)$$

and therefore $\alpha \approx d - D$. The authors show that if t is small enough, this estimate is accurate.

This procedure can be seen as approximating the asymptotic slope of the parametric curve $(\log \sqrt{t}, \log \rho_t(x))$, or in other words, the graph of $s \mapsto \log \rho_{e^{2s}}(x)$ for $s \rightarrow -\infty$. Another approach would be to study the derivative of this function. Let us define

$$\beta_t(x) = \frac{2t}{\rho_t(x)} \frac{d}{dt} \rho_t(x) = \frac{t}{\rho_t(x)} \Delta \rho_t(x), \quad (12)$$

where the last equality comes from the diffusion equation (1). Moreover, denote the asymptotic slope of the aforementioned curve by

$$\beta(x) = \lim_{s \rightarrow -\infty} \frac{d}{ds} \log \rho_{e^{2s}}(x) = \lim_{t \rightarrow 0^+} \beta_t(x). \quad (13)$$

The next proposition will enable us to conclude that indeed these two approaches are equivalent.

Proposition 5.1. *Given a strictly positive differentiable function $f: (0, a) \rightarrow (0, \infty)$ and a positive real number $\alpha > 0$, the following conditions are equivalent.*

1. *The function f explodes at 0 like $t^{-\alpha}$, i.e. for some positive constants $c, C > 0$ one has $c < t^\alpha f(t) < C$ for some $\epsilon > 0$ and $t \in (0, \epsilon)$.*
2. $\log f(t) = -\alpha \log t + O(1)$.
3. $\lim_{t \rightarrow 0^+} \log f(t) / \log t = -\alpha$.
4. $\lim_{t \rightarrow 0^+} t f'(t) / f(t) = -\alpha$.

Proof. All limits will be taken with $t \rightarrow 0$, and we will omit this from notation.

If $t < t^\alpha f(t) < C$, then $\log(t^\alpha f(t)) = O(1)$. Rearranging leads to point 2. Going further, dividing by $\log x$ and observing that $\lim O(1) / \log t = 0$ yields point 3.

Now, assume condition 3. Since $\lim \log t = -\infty$, for the whole expression to tend to $-\alpha < 0$, we need $\lim \log f(t) = \infty$. In this case however we may apply the de l'Hospital rule giving rise to point 4.

It remains to show the final implication. Let $g(t) = t^\alpha f(t) > 0$ be the function we want to bound. Substituting $f(t) = t^{-\alpha}g(t)$ into $\lim_{t \rightarrow 0} tf'(t)/f(t) = -\alpha$, we obtain

$$\lim \frac{t(-\alpha t^{-\alpha-1}g(t) + t^{-\alpha}g'(t))}{t^{-\alpha}g(t)} = \lim \left(-\alpha + \frac{g'(t)}{g(t)} \right) = -\alpha, \quad (14)$$

amounting to $\lim(\log g(t))' = 0$. But this means that for some $\epsilon > 0$, the derivative $(\log g(t))'$ is bounded on $(0, \epsilon)$, implying that $\log g(t)$ is Lipschitz and therefore bounded on this interval. This yields the desired estimates. \square

Now, by putting $f(t) = \rho_t(x)$, we can see that the last condition of Proposition 5.1 holds with $\alpha = -\beta(x)/2$. Thus, the equivalent condition 2. yields the following equivalence of both presented approaches.

Corollary 5.2. *For t near 0 the following estimate holds*

$$\log \rho_t(x) = \beta(x) \log \sqrt{t} + O(1). \quad (15)$$

As a consequence, the estimation of Local Intrinsic Dimension using LIDL can be achieved by computing $\beta(x)$, yielding $d = D + \beta(x)$.

The next proposition provides an elegant expression for $\beta_t(x)$, and consequently for $\beta(x)$, expressed in terms of the density ψ on \mathbb{R}^d .

Proposition 5.3. *For $t > 0$ and $x \in S = \mathbb{R}^d \subseteq \mathbb{R}^D$ we have*

$$\beta_t(x) = d - D + \frac{\Delta_x(\psi * \phi_t^d)(x)}{\psi * \phi_t^d(x)} \cdot t. \quad (16)$$

Proof. Since ρ_t is the solution of the diffusion equation on \mathbb{R}^D with $C = 1/2$, we can replace the time derivative with $\Delta/2$, obtaining by Lemma 4.1

$$\beta_t(x) = \frac{2t}{\rho_t(x)} \frac{d}{dt} \rho_t(x) = \frac{t}{\rho_t(x)} \Delta \rho_t(x) = d - D + \frac{t(2\pi t)^{(d-D)/2} \Delta_x(\psi * \phi_t^d)(x)}{\rho_t(x)}, \quad (17)$$

where in the second term $(2\pi t)^{(d-D)/2}$ cancels out after expanding ρ_t in the denominator. \square

5.1 Examples

From the theoretical considerations in Tempczyk et al. (2022) it follows, that $\beta(x) = d - D$ if ψ is sufficiently regular and positive near x . In other words, in this case

$$\lim_{t \rightarrow 0^+} \frac{\psi * \Delta \phi_t^d(x)}{\psi * \phi_t^d(x)} \cdot t = 0. \quad (18)$$

In this section, we will try to obtain this conclusion directly in a few special cases by analyzing the behavior of $\beta_t(x)$.

The “uniform distribution” on Euclidean space Clearly, there is no such thing as the uniform distribution on \mathbb{R}^d . However, from a purely theoretical viewpoint, in our differential equation approach we don't need the assumption of ϕ being a probability density; it could be any function. And since constant functions are usually the simplest examples, we will now investigate what happens if we put $\psi(x) \equiv 1$ on the whole \mathbb{R}^d space.

Using Proposition 5.3 and the fact that ψ has bounded derivatives, this case leaves us with

$$\beta_t(x) = d - D + \frac{\Delta_x \psi * \phi_t^d(x)}{\psi * \phi_t^d(x)} \cdot t = d - D, \quad (19)$$

since $\Delta_x \psi \equiv 0$. This expression is constant in t , and in particular its limit at 0 is $\beta(x) = d - D$. In this case LIDL estimator is not biased for all $t > 0$.

Normal distribution Let us now consider the normal distribution on \mathbb{R}^d with covariance matrix $\Sigma = \text{diag}(\sigma_1^2, \dots, \sigma_d^2)$, and denote its density function by ψ . The convolution $\psi * \phi_t^d$ is the density of the normal distribution with covariance matrix $\Sigma + tI$. If we simplify notation by putting $\phi_i = \phi_{\sigma_i^2+t}^1$, we get

$$\psi * \phi_t^d(x) = \prod_{i=1}^d \phi_i(x_i). \quad (20)$$

To compute the Laplacian of this convolution, note that

$$\psi * \phi_t^d(x) = \frac{\psi * \phi_t^d(x)}{\phi_i(x_i)} \cdot \phi_i(x_i), \quad (21)$$

where the first factor does not depend of x_i , and therefore

$$\frac{\partial^2(\psi * \phi_t^d)}{\partial x_i^2}(x) = \psi(x) * \phi_t^d(x) \cdot \frac{1}{\phi_i(x_i)} \frac{\partial^2 \phi_i}{\partial x_i^2}(x_i), \quad (22)$$

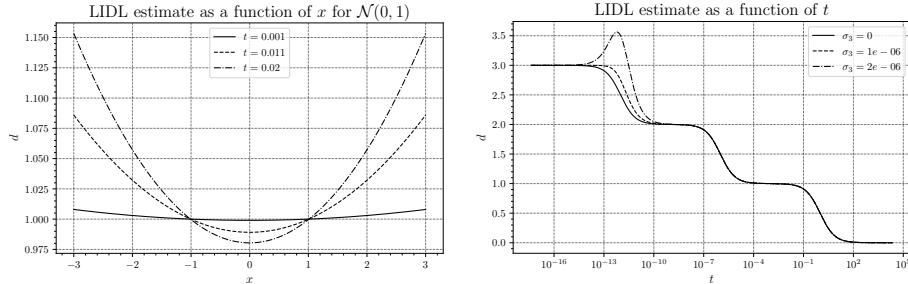
leading to

$$\beta_t(x) = d - D + t \frac{\Delta(\psi * \phi_t^d)(x)}{\psi * \phi_t^d(x)} = d - D + t \sum_{i=1}^d \frac{1}{\phi_i(x_i)} \frac{\partial^2 \phi_i}{\partial x_i^2}(x_i) = d - D + t \sum_{i=1}^d \frac{x_i^2 - (\sigma_i^2 + t)}{(\sigma_i^2 + t)^2}. \quad (23)$$

It is easy to see that the second derivatives of ϕ_i are continuous in $t > -\sigma_i^2$, so the sum in the above expression has finite limit for $t \rightarrow 0$, and therefore $\beta(x) = d - D$.

In the special case where $\Sigma = \sigma^2 I$, these calculations simplify further, as $\psi * \phi_t^d = \phi_{\sigma^2+t}^d$, and since

$$\Delta_x \phi_{\sigma^2+t}^d(x) = \left(\frac{\|x\|^2}{(\sigma^2 + t)^2} - \frac{d}{\sigma^2 + t} \right) \phi_{\sigma^2+t}^d(x), \quad (24)$$



(a) Example of the bias of a LIDL estimate for different points from $\mathcal{N}(0,1)$ and for different values of t . This plot recreates a numerical calculations presented in Figure 4 from Tempczyk et al. (2022). (b) Plot of a LIDL estimate as a function of time for 3-dimensional Gaussian distribution with $\Sigma = \text{diag}(1, 10^{-6}, 10^{-12})$ and for three different points $x = (0, 0, \sigma_3)$, which represents a different distance from 0.

Figure 1: Deviations from desired LID estimates for Gaussian distributions.

we have

$$\beta_t(x) = d - D + \left(\frac{\|x\|^2}{(\sigma^2 + t)^2} - \frac{d}{\sigma^2 + t} \right) t. \quad (25)$$

These results express analytically experimental observations from LIDL and FLIPD papers, which we show in Fig. 1. We can also observe, that if we move to the regions of very low probability for a Gaussian, it generates very high positive bias, which may highly overestimate the true LID. Luckily, most of the points in our dataset comes from the region of high probability, but we should be less certain of the estimates for points from low probability regions.

Arbitrary distribution with sufficiently nice density By this point it should already be clear what a nice density is. We want to be able to use the equality $\Delta_x(\psi * \phi_t^d) = \Delta_x\psi * \phi_t^d$. In order to do so, we need ψ to be bounded, twice differentiable, and have bounded first and second-order partial derivatives. Moreover, we will require ψ to have *continuous* second-order partial derivatives. This is not very restrictive, and many distributions satisfy these properties, including the normal distribution or more generally, mixtures of Gaussians.

In this case, we have

$$\beta_t(x) = d - D + \frac{\Delta_x\psi * \phi_t^d(x)}{\psi * \phi_t^d(x)} \cdot t, \quad (26)$$

however this time $\Delta_x\psi$ is some arbitrary continuous function. Being differentiable, ψ is also continuous, and we can use the general fact that for a bounded continuous function, f on \mathbb{R}^d one has

$$\lim_{t \rightarrow 0^+} f * \phi_t^d(x) = f(x). \quad (27)$$

This gives us, for x such that $\psi(x) > 0$,

$$\lim_{t \rightarrow 0^+} \frac{\Delta_x \psi * \phi_t^d}{\psi * \phi_t^d} \cdot t = \frac{\Delta_x \psi(x)}{\psi(x)} \lim_{t \rightarrow 0^+} t = 0, \quad (28)$$

and again $\beta(x) = d - D$. We have proven that in this case β yields a correct estimate of dimension, circumventing all the complexities of the proofs in Tempczyk et al. (2022).

It is worth noting, that when $\Delta_x \psi = 0$, the estimate is accurate. It is the case for the aforementioned "uniform distribution" on \mathbb{R}^d , but it is also true if locally the density is a linear function of x . In Fig. 1a we can observe, that for $x \approx \pm 1$ and small values of t , the estimate is accurate.

6 Conclusions

In this work, we have outlined a new perspective for Wiener process based algorithms for LID estimation and shown some results for LIDL, in which we find an analytical description for the phenomena observed in experiments. The future directions from here are: analyzing the uniform distribution on a line segment, adding curvature to this analysis, and an attempt to analyze an NB algorithm in the same way as LIDL.

7 Acknowledgements

Some experiments were performed using the Entropy cluster at the Institute of Informatics, University of Warsaw, funded by NVIDIA, Intel, the Polish National Science Center grant UMO2017/26/E/ST6/00622, and ERC Starting Grant TOTAL. The rest of the experiments were performed using the GUŚLARZ 9000 workstation at the Polish Lab for AI (PL4AI).

We want to thank Marek Cygan and Adam Goliński for their overall support during this project.

CRediT Author Statement

Piotr Tempczyk (35% of the work): Conceptualization, Methodology, Software, Validation, Formal analysis, Investigation, Data Curation, Writing - Original Draft, Writing - Review & Editing, Visualization, Supervision, Project administration.

Adam Kurpisz (30% of the work): Conceptualization, Methodology, Validation, Formal analysis, Investigation, Writing - Original Draft, Writing - Review & Editing, Visualization, Supervision.

Łukasz Garncarek (25% of the work): Conceptualization, Methodology, Formal analysis, Investigation, Writing - Original Draft, Writing - Review & Editing.

Dominik Filipiak (10% of the work): Software, Data Curation.

References

- A. Ansuini, A. Laio, J. H. Macke, and D. Zoccolan. Intrinsic dimension of data representations in deep neural networks. In *Advances in Neural Information Processing Systems*, pages 6111–6122, 2019.
- J. Bailey, M. E. Houle, and X. Ma. Local intrinsic dimensionality, entropy and statistical divergences. *Entropy*, 24(9):1220, 2022.
- J. Bailey, M. E. Houle, and X. Ma. Relationships between tail entropies and local intrinsic dimensionality and their use for estimation and feature representation. *Information Systems*, 118:102245, 2023.
- B. C. Brown, A. L. Caterini, B. L. Ross, J. C. Cresswell, and G. Loaiza-Ganem. Verifying the union of manifolds hypothesis for image data. In *The Eleventh International Conference on Learning Representations*, 2022.
- F. Camastra and A. Staiano. Intrinsic dimension estimation: Advances and open problems. *Information Sciences*, 328:26–41, 2016.
- P. Campadelli, E. Casiraghi, C. Ceruti, and A. Rozza. Intrinsic dimension estimation: Relevant techniques and a benchmark framework. *Mathematical Problems in Engineering*, 2015:1–21, 2015.
- M. Fan, N. Gu, H. Qiao, and B. Zhang. Intrinsic dimension estimation of data by principal component analysis. *arXiv preprint arXiv:1002.2050*, 2010.
- K. Fukunaga and D. R. Olsen. An algorithm for finding intrinsic dimensionality of data. *IEEE Transactions on Computers*, C-20:176–183, 1971. URL <https://api.semanticscholar.org/CorpusID:30206700>.
- C. Horvat and J.-P. Pfister. Intrinsic dimensionality estimation using normalizing flows. *Advances in Neural Information Processing Systems*, 35:12225–12236, 2022.
- C. Horvat and J.-P. Pfister. On gauge freedom, conservativity and intrinsic dimensionality estimation in diffusion models. *arXiv preprint arXiv:2402.03845*, 2024.
- K. Johnsson, C. Soneson, and M. Fontes. Low bias local intrinsic dimension estimation from expected simplex skewness. *IEEE transactions on pattern analysis and machine intelligence*, 37(1):196–202, 2014.

- H. Kamkari, B. L. Ross, J. C. Cresswell, A. L. Caterini, R. G. Krishnan, and G. Loaiza-Ganem. A geometric explanation of the likelihood ood detection paradox. *arXiv preprint arXiv:2403.18910*, 2024a.
- H. Kamkari, B. L. Ross, R. Hosseinzadeh, J. C. Cresswell, and G. Loaiza-Ganem. A geometric view of data complexity: Efficient local intrinsic dimension estimation with diffusion models. *arXiv e-prints*, pages arXiv–2406, 2024b.
- M. Kleindessner and U. Luxburg. Dimensionality estimation without distances. In *Artificial Intelligence and Statistics*, pages 471–479, 2015.
- E. Levina and P. Bickel. Maximum likelihood estimation of intrinsic dimension. *Advances in neural information processing systems*, 17, 2004.
- C. Li, H. Farkhoor, R. Liu, and J. Yosinski. Measuring the intrinsic dimension of objective landscapes. In *International Conference on Learning Representations*, 2018.
- G. Loaiza-Ganem, B. L. Ross, R. Hosseinzadeh, A. L. Caterini, and J. C. Cresswell. Deep generative models through the lens of the manifold hypothesis: A survey and new connections. *arXiv preprint arXiv:2404.02954*, 2024.
- T. Minka. Automatic choice of dimensionality for pca. *Advances in neural information processing systems*, 13, 2000.
- P. Pope, C. Zhu, A. Abdelkader, M. Goldblum, and T. Goldstein. The intrinsic dimension of images and its impact on learning. In *International Conference on Learning Representations*, 2020.
- P. K. Rubenstein, B. Schoelkopf, and I. Tolstikhin. On the latent space of wasserstein auto-encoders. *arXiv preprint arXiv:1802.03761*, 2018.
- Y. Song, J. Sohl-Dickstein, D. P. Kingma, A. Kumar, S. Ermon, and B. Poole. Score-based generative modeling through stochastic differential equations. In *International Conference on Learning Representations*, 2020.
- J. P. Stanczuk, G. Batzolis, T. Deveney, and C.-B. Schönlieb. Diffusion models encode the intrinsic dimension of data manifolds. In *International Conference on Machine Learning*, 2024.
- P. Tempczyk, R. Michaluk, L. Garncarek, P. Spurek, J. Tabor, and A. Golinski. Lidl: Local intrinsic dimension estimation using approximate likelihood. In *International Conference on Machine Learning*, pages 21205–21231. PMLR, 2022.
- V. Vapnik. *The nature of statistical learning theory*. Springer science & business media, 2013.
- E. Yeats, C. Darwin, F. Liu, and H. Li. Adversarial estimation of topological dimension with harmonic score maps. *arXiv preprint arXiv:2312.06869*, 2023.

Y. Zheng, T. He, Y. Qiu, and D. P. Wipf. Learning manifold dimensions with conditional variational autoencoders. *Advances in Neural Information Processing Systems*, 35:34709–34721, 2022.